

DETERMINATION OF OPTICALLY STIMULATED LUMINESCENCE  
DOSIMETRIC CHARACTERISTICS AND SUITABILITY FOR ENTRANCE  
SURFACE DOSE ASSESSEMENT IN DIAGNOSTIC X-RAY EXAMINATIONS

YAHAYA MUSA

A thesis submitted in fulfilment of the  
requirements for the award of the degree of  
Doctor of Philosophy

Faculty of Science  
Universiti Teknologi Malaysia

NOVEMBER 2018

## **DEDICATION**

This thesis is dedicated to my parents  
Late Alhaji Musa Danladi and Hajiya Maryam Muhammad Lukman.

## ACKNOWLEDGEMENT

First, I thank Allah, the almighty for giving me the wisdom and strength to carry out this research. I would like to express my sincere gratitude and appreciation to my supervisor, Assoc. Prof. Dr. Suhairul Bin Hashim for his endless support, guidance, patience and encouragement. His inspiration and guidance helped me realize my potentials and proved to be the decisive element to the success of this research. I would like to extend my sincere gratitude to my co-supervisor, Dr Nor Ezzaty Ahmad for her generous guidance and support, her contributions to make this research possible cannot be overstated.

My sincere appreciation goes to the entire technical staff of Nuclear Lab, department of Physics for their guidance and tolerance throughout the experimental works. I am grateful to my research group members: Dr. Muhammad Khalis Abdul Karim, Dr. Muhammad Abu Mhareb, Nasuha Salehhon, Ang Wee Chin, Ratna Suffhiyanni Omar, Asmah Bohari and Andrew Ochoji. I am also grateful to my colleagues Dr. N.N. Garba, Dr. Y. A. Yamusa, A.U. Abubakar, Dr. Aminu Ismail, Salihu Dishing, Bashir Jatau, Dr. Suraj Suleiman and many others for their support during this journey.

I would like to acknowledge with gratitude, the love and support of my entire family. To my late father, your boundless love and support will always remain with me. May Allah accept this as an act charity and send light to your grave. I am grateful to my mother, your unending love and support throughout my life have always given me confidence to the next level. To my brothers and sister, you have always supported me at difficult times, thank you. I am also grateful to specially; Salihu Muhammed Lukman and Dr Salihu Lukman for being helpful when I needed it the most. I am also grateful to my beloved wife for her sacrifice, considerate and being supportive throughout this journey. You all kept me going, and this thesis would not have been possible without you.

This thesis turns out to be a reality with the kind support of many individuals that could not be mentioned here. I would like to extend my sincere appreciations to all of them.

I am thankful to the management of Centre for Energy Research and Training, Ahmadu Bello University, Zaria for kind approval to my study fellowship application.

Finally, I am thankful to Ahmadu Bello University, Zaria for providing the financial support through the Needs Assessment and Intervention Fund.

## ABSTRACT

The availability of Optically Stimulated Luminescence (OSL) dosimeter system developed by Landauer Inc. (Glenwood IL) has greatly improved radiation dosimetry application in the medical field. Recent studies with OSL dosimeters (nanoDots) gave much emphases to patient radiation exposure in radiotherapy but ignoring the potential risks from radiographic examinations. This study focused on the measurement of entrance surface dose (ESD) resulting from radiographic examination. Monitoring procedures have been developed by the International Atomic Energy Agency (IAEA) to estimate ESD, while considering exposure parameters and patient's characteristics. However, dosimetric properties of the OSL system must be characterized to ascertain its suitability for ESD measurements in medical radiography due to energy dependence and over-response factors of the  $\text{Al}_2\text{O}_3$  material. This thesis consists of three phases: 1) evaluating stability of the new OSL dosimetry system, 2) characterizing the nanoDots in radiographic energy range from 40 kV to 150 kV with typical doses ranging from 0 to 20 mGy, and 3) assessing suitability of the nanoDots for ESD measurement in routine X-ray examinations. The dosimetric characteristics of the nanoDots in the above energy range are presented in this study, including repeatability, reproducibility, signal depletion, element correction factor, linearity, angular and energy dependence, and dose measurement accuracy. Experimental results showed repeatability of below 5% and reproducibility of less than 2%. OSL signals after sequential readouts were reduced by approximately 0.5% per readout and having good linearity for doses between 5 – 20 mGy. The nanoDots OSL dosimeter showed significant angular and energy dependence in this energy range, and corresponding energy correction factors were determined in the range of 0.76 – 1.12. ESDs were determined in common diagnostic X-ray examinations using three different methods including direct (measured on phantom/patient) and indirect (without phantom) measurements with nanoDots OSL dosimeters, and CALDose\_X 5.0 software calculations. Results from direct and indirect ESD measurements showed good agreement within relative uncertainties of 5.9% and 12%, respectively, in accordance with the International Electrotechnical Commission (IEC) 61674 specifications. However, the measured results were below ESDs calculated with CALDose\_X 5.0 software. Measured eye and gonad doses were found to be significant compared to ESDs during anterior-posterior (AP) abdomen and AP skull examinations, respectively. The results obtained in this research work indicate the suitability of utilizing nanoDots OSL dosimeter for entrance surface dose assessment during diagnostic X-ray examinations.

## ABSTRAK

Ketersediaan dosimeter OSL (Optically Stimulated Luminescence) yang dikembangkan oleh Landauer Inc. (Glenwood IL) telah menambah baik aplikasi dosimetri sinaran dalam bidang perubatan. Kajian terbaharu dengan dosimeter OSL (nanoDots) memberi lebih penekanan kepada dedahan sinaran terhadap pesakit dalam radioterapi tetapi mengabaikan potensi risiko daripada pemeriksaan radiografi. Kajian ini memberi tumpuan kepada pengukuran dos permukaan masuk (ESD) yang terhasil daripada pemeriksaan radiografi. Prosedur pemantauan telah dikembangkan oleh Agensi Tenaga Atom Antarabangsa (IAEA) untuk menganggarkan ESD, sambil mempertimbangkan parameter dedahan dan ciri-ciri pesakit. Walau bagaimanapun, sifat dosimetri sistem OSL mesti dicirikan untuk menentukan kesesuaiannya bagi pengukuran ESD dalam radiografi perubatan disebabkan oleh faktor kebersandaran tenaga dan lampau-sambutan oleh bahan  $Al_2O_3$ . Tesis ini merangkumi tiga fasa: 1) menilai kestabilan sistem OSL yang baharu, 2) pencirian nanoDots dalam julat tenaga radiografi daripada 40 kV sehingga 150 kV dengan dos tipikal daripada 0 sehingga 20 mGy, dan 3) menilai kesesuaian nanoDots bagi pengukuran ESD dalam pemeriksaan sinar-X rutin. Ciri-ciri dosimetri nanoDots dalam julat tenaga di atas dibentangkan dalam kajian ini, termasuk keterulangan, kebolehulangan semula, penyusutan isyarat, faktor pembetulan unsur, kelinearan, kebersandaran sudut dan tenaga, dan kejituan pengukuran dos. Dapatan eksperimen menunjukkan keterulangan adalah di bawah 5% dan kebolehulangan semula adalah kurang daripada 2%. Isyarat OSL selepas bacaan berjujukan berkurang kira-kira 0.5% setiap kali bacaan dan mempunyai kelinearan baik untuk dos di antara 5 - 20 mGy. Dosimeter OSL nanoDots menunjukkan kebersandaran sudut dan tenaga yang ketara dalam julat tenaga ini, dan faktor pembetulan tenaga yang sepadan ditentukan dalam julat 0.76 - 1.12. ESD ditentukan dalam pemeriksaan diagnosis sinar-X menggunakan tiga kaedah yang berbeza termasuk pengukuran langsung (diukur pada fantom/pesakit) pengukuran tidak langsung (tanpa fantom) dengan dosimeter OSL nanoDots, dan pengiraan menggunakan perisian CALDose\_X 5.0. Keputusan dari pengukuran ESD secara langsung dan tidak langsung menunjukkan persetujuan yang baik dalam ketidakpastian relatif masing-masing sebanyak 5.9% dan 12%, selaras dengan spesifikasi Suruhanjaya Elektroteknikal Antarabangsa (IEC) 61674. Bagaimanapun, dapatan terukur adalah di bawah ESD yang dikira menggunakan perisian CALDose\_X 5.0. Dos terukur di mata dan gonad didapati lebih ketara berbanding dengan ESD yang diukur semasa pemeriksaan abdomen anterior-posterior (AP) dan tengkorak AP. Keputusan yang diperolehi dalam kajian ini menunjukkan kesesuaian menggunakan dosimeter OSL nanoDots untuk penilaian dos permukaan masuk semasa pemeriksaan diagnostik sinar- X.

## TABLE OF CONTENTS

	<b>TITLE</b>	<b>PAGE</b>
	<b>DECLARATION</b>	<b>ii</b>
	<b>DEDICATION</b>	<b>iii</b>
	<b>ACKNOWLEDGEMENT</b>	<b>iv</b>
	<b>ABSTRACT</b>	<b>v</b>
	<b>ABSTRAK</b>	<b>vi</b>
	<b>TABLE OF CONTENTS</b>	<b>vii</b>
	<b>LIST OF TABLES</b>	<b>xi</b>
	<b>LIST OF FIGURES</b>	<b>xiii</b>
	<b>LIST OF ABBREVIATIONS</b>	<b>xviii</b>
	<b>LIST OF SYMBOLS</b>	<b>xx</b>
	<b>LIST OF APPENDICES</b>	<b>xxii</b>
<b>CHAPTER 1</b>	<b>INTRODUCTION</b>	<b>1</b>
1.1	Background of the Research	1
1.2	Problem Statements	3
1.3	Aim and Objectives of the Research	7
1.4	Scope of the Research	7
1.5	Thesis Outline	8
<b>CHAPTER 2</b>	<b>LITERATURE REVIEW</b>	<b>10</b>
2.1	X-rays and their applications in diagnostic radiology	10
2.1.1	X-ray production	11
2.1.1.1	General radiography	12
2.1.1.2	Dual-energy subtraction radiography	13
2.1.2	Interaction of photons with matter	14
2.1.2.1	Rayleigh scattering	15
2.1.2.2	Photoelectric absorption	16

	2.1.2.3	Compton effect	18
	2.1.2.4	Pair production	20
2.2		Luminescence	21
2.3		Optically stimulated luminescence (OSL)	23
	2.3.1	Continuous-wave OSL (CW-OSL)	26
	2.3.2	Pulsed OSL (POSL)	27
	2.3.3	Linear modulated OSL (LM-OSL)	28
2.4		Optically stimulated luminescence dosimetry with $\text{Al}_2\text{O}_3:\text{C}$	29
2.5		OSL dosimetric characteristics	33
	2.5.1	Reproducibility	34
	2.5.2	Dose response	36
	2.5.3	Energy dependence	38
	2.5.4	Angular dependence	39
	2.5.5	Sensitivity	41
	2.5.6	OSL signal depletion	42
	2.5.7	Element correction factor (ECF)	43
2.6		Definition of terms	44
	2.6.1	Absorbed dose	44
	2.6.2	Dose equivalent	45
	2.6.3	Incidence air kerma	46
	2.6.4	Entrance surface Dose	46
	2.6.5	X-ray tube output	47
	2.6.6	Tube current	47
	2.6.7	Tube potential	47
	2.6.8	Field size	48
	2.6.9	Patient size	48
	2.6.10	Radiographic positioning terminologies and projections	48
	2.6.11	Stochastic effects	49
2.7		Phantoms	49
	2.7.1	Anthropomorphic phantom for X-ray imaging	50
2.8		Dosimetry survey	53

2.8.1	Entrance surface dose (ESD) estimation	53
2.8.2	Diagnostic Reference Levels (DRLs) for general radiography	60
<b>CHAPTER 3</b>	<b>RESEARCH METHODOLOGY</b>	<b>62</b>
3.1	Introduction	62
3.1.1	OSL dosimeter (nanoDot)	62
3.1.2	Pocket annealer	64
3.1.3	MicroStar reader	64
3.1.4	MicroStar software	66
3.1.5	X-ray generators	67
3.1.6	Ionization chamber	70
3.2	Methodology	72
3.2.1	Reader stability test	73
3.2.2	Reader calibration	73
3.3	Dosimetry characterization	74
3.3.1	Repeatability	75
3.3.2	Reproducibility	77
3.3.3	Dose response	77
3.3.4	Energy dependence	78
3.3.5	Angular dependence	79
3.3.6	OSL signal depletion	80
3.3.7	Element correction factor ( <i>ECF</i> )	80
3.3.8	Dose measurement accuracy	80
3.4	Entrance surface dose (ESD) evaluation	81
3.4.1	Indirect ESD measurements	82
3.4.2	Direct ESD measurements	83
3.4.3	ESD calculations with CALDose_X 5.0 software	84
3.4.4	ESD measurement in dual-energy radiography	85
<b>CHAPTER 4</b>	<b>RESULTS AND DISCUSSION</b>	<b>87</b>
4.1	Introduction	87
4.2	Reader performance evaluation	87



4.2.1	Reader stability test	88
4.2.2	Reader calibration	91
4.3	Dosimetric characterization	96
4.3.1	Repeatability	96
4.3.2	Reproducibility	100
4.3.3	Dose response	103
4.3.3.1	Linearity test with Philips Industrial X-ray unit	104
4.3.3.2	Linearity test with Siemens Multix top X-ray unit	107
4.3.4	Energy dependence	110
4.3.5	Angular dependence	114
4.3.6	OSL signal depletion	116
4.3.7	Element correction factors ( <i>ECF</i> )	117
4.3.8	Dose measurement accuracy	119
4.4	Entrance surface dose (ESD)	122
4.4.1	Entrance surface dose evaluations in general radiography	122
4.4.2	Entrance surface dose measurement in dual energy radiography	137
<b>CHAPTER 5</b>	<b>CONCLUSION AND RECOMMENDATIONS</b>	<b>144</b>
5.1	Conclusion	144
5.2	Recommendations	147
	<b>REFERENCES</b>	<b>150</b>
	<b>LIST OF PUBLICATIONS</b>	<b>168</b>

## LIST OF TABLES

TABLE NO.	TITLE	PAGE
2.1	Photon energy ranges from diagnostic to radiotherapy (Chang et al., 2014).	12
2.2	Historical advancement of OSL dosimetry.	32
2.3	Previous studies on reproducibility of Al <sub>2</sub> O <sub>3</sub> :C dosimeters in different beams.	35
2.4	Comparison of dose response from previous studies.	38
2.5	Recent findings on Al <sub>2</sub> O <sub>3</sub> :C OSL dosimeter dependence on energy.	39
2.6	Variation of angular dependence data with respect to different photon beams.	40
2.7	Recent findings on Al <sub>2</sub> O <sub>3</sub> :C OSL dosimeter signal depletion.	42
2.8	Highlight of previous studies on ESD estimation in diagnostic radiology.	56
2.9	Highlight of some previous ESD evaluation in common X-ray examinations.	58
2.10	Comparison of current established DRLs for common adult radiographic examinations from different countries.	61
3.1	MicroStar software features	67
3.2	X-ray generators used in this study for OSLD characterization and ESD measurements.	69
3.3	Exposure parameters using RQR radiation qualities.	76
3.4	Details of the IEC 61267 codes for RQR radiation qualities at 100 cm from the focal spot.	79
3.5	Measurement scenarios of ESD for the X-ray examinations using OSLDs.	82
3.6	List of CALDose_X 5.0 software input parameters used for entrance surface dose calculations.	84
4.1	Coefficient of variation (CV) test for the microStar reader.	91
4.2	Average counts, standard deviation (SD) and coefficient of variation (CV) of dosimeters having maximum and	

	minimum CVs among the ten nanoDots irradiated for each tube voltage. The maximum and minimum CVs represent the repeatability range of nanoDots in the selected doses and radiation qualities.	97
4.3	The energy response factors comparison between the OSLDs and TLD-100, where $\Delta$ (%) is the percentage difference relative to 80 kV irradiations.	114
4.4	Exposure parameters used for all projections.	123
4.5	Measured and calculated ESD distribution with their associated uncertainties in different projections.	125
4.6	Values of mean ESD, standard deviation (SD) and coefficient of variation (CV) of ESD for the various projections.	130
4.7	Comparison of ESDs with previously reported values in the literature.	132
4.8	Entrance dose to the eye, thyroid and gonad measured directly with OSLDs placed on the surface during the selected examinations.	133
4.9	Comparison of ESDs achieved by the present work with established international DRLs.	136
4.10	Exposure parameters and ESD distribution of the thirty patients examined for chest radiography with single-shot and dual-shot.	139

## LIST OF FIGURES

FIGURE NO.	TITLE	PAGE
1.1	Schematic diagram of the research problem statement.	6
2.1	X-ray image of balance-weights in a closed box and shotgun by Rontgen in 1896 (Mery 2015).	10
2.2	Image of supine AP abdomen radiograph showing the patient's anatomy, with S and d representing the stomach and duodenum (Brant and Clyde, 2007).	13
2.3	Comparison of normal chest X-ray with a soft tissue and with rib shadows eliminated (Manji et al., 2016).	14
2.4	Rayleigh scattering in which a photon is released with the same energy as the incident photon.	16
2.5	Illustration of photoelectric effect with incident photon completely transferring its energy to the photoelectron.	17
2.6	Dependence of photoelectric coefficient on (a) atomic number and (b) photon energy.	18
2.7	The Compton scattering.	19
2.8	The three mechanisms of photon interaction relative to the values of Z and photon energy.	20
2.9	Schematic representation of optically stimulated luminescence (Yukihara and McKeever, 2008).	23
2.10	Schematic diagram of the CW-OSL stimulation mode (Bøtter-Jensen, McKeever, and Wintle 2003).	26
2.11	Schematic representation of the POSL mode (Bøtter-Jensen, McKeever, and Wintle 2003).	27
2.12	Schematic diagram of the LM-OSL stimulation mode (Bøtter-Jensen, McKeever, and Wintle 2003).	28
2.13	Comparison of CW-OSL and LM-OSL monitored signal decay (Yukihara and McKeever 2011).	29
2.14	Al <sub>2</sub> O <sub>3</sub> :C in crystal and powder form (Yukihara and McKeever 2011).	30
2.15	Schematic diagram of basic OSL process (Yukihara and McKeever 2011).	31
2.16	Dose response characteristics of typical dosimeters.	37

2.17	(a) RANDO Man phantom (b) RANDO Woman phantom.	51
2.18	Alderson Rando phantom (b) Skull 3M phantom and (c) Alderson chest and lung phantom with removable diaphragm.	52
2.19	(a) and (b) are multipurpose chest phantom Kyoto Kagaku “LUNGMAN” with chest plate and its inner components respectively. (c) Whole body phantom Kyoto Kagaku PBU-50.	53
3.1	InLight nanoDots dosimeter	63
3.2	Pocket annealer for bleaching InLight OSL dosimeters.	64
3.3	Schematic diagram of the working processes of microStar reader.	65
3.4	Front view of the microStar reader.	66
3.5	(a) Siemens Multix top model X-ray generator for OSLD irradiations in free air (b) GE Digital Rad X-ray generator set up for ESD measurements on anthropomorphic phantom.	68
3.6	Setting up Philips Industrial X-ray for exposure to RQR radiation qualities for energy range 40 – 150 kV.	70
3.7	Unidos electrometer (T10002) with ionization chamber.	71
3.8	Chart of methodology	72
3.9	Schematic diagram depicting the irradiation setup of the nanoDots characterization with Philips Industrial X-ray unit.	74
3.10	Irradiation setup for OSLD characterization with Philip industrial X-ray unit.	75
3.11	Measurement cycle involving irradiation-readout-annealing.	77
3.12	Exposure set-up for direct and indirect ESD measurements. NanoDots were placed in free air and in the absence of backscatter material (phantom) to measure incident air kerma for indirect ESD evaluation. While nanoDots placed on phantom/patient surface were used for direct ESD measurements.	83
3.13	Image of AP abdomen view of phantom with location and field size from the CALDose_X 5.0 software.	85
4.1	Mean DRK counts for 10 consecutive days with error bars representing the standard deviation of the mean. Each data point represents the average of ten repeated measurements	

	performed per day, and the dotted line denotes the control limit of DRK count (<30).	88
4.2	The distribution of reader background signal in terms of CAL and LED counts measured for 10 consecutive days. Each data point represents the average of ten repeated measurements performed per day.	89
4.3	Variations of CAL and LED counts showing their deviation from the mean of hundred measurements performed within 10 days.	90
4.4	Dose linearity calibration curve and associated coefficient of variation. There are five data points at 0, 5, 30, 500 and 1000 mGy, with points at 0, 5, and 30 mGy representing low dose calibration, and 0, 500, 1000 mGy representing high dose calibration.	92
4.5	The combined two dynamic ranges obtained from calibration of the microStar reader having low-dose calibration in the range 0 – 30 mGy (low-dose region) and high-dose calibration in the range 0 – 1000 mGy (high-dose region). Each region has its own mode of stimulation to balance the uncertainty due to difference in level of stimulation separated by cross-over point represented by dotted line.	93
4.6	The PMT counts is curved due to transition of the stimulation mode from strong beam (low dose) to weak beam (high dose) just before the dotted line (cross-over point). While the associated counting errors decrease with increasing dose. The trend of this fitted curve is in good agreements with the manufacturer’s dynamic range curve published earlier (Yahnke, 2009).	95
4.7	Distribution of repeated readouts for selected dosimeters exposed to different doses for 80 kVp X-ray. Majority of the readings are centred within $\pm 2\%$ of the mean, which represent 60%, 100% and 80% of the data for 5 mGy, 8 mGy and 20 mGy respectively.	98
4.8	Repeatability of nanoDots irradiated to unknown doses with Siemens model X-ray unit. Each data point represents the CV of ten repeated readings, while the error bars denote the standard deviation.	99
4.9	Reproducibility of individual nanoDots following irradiation-reading-annealing cycle.	101
4.10	Corresponding doses of the nanoDots reproducibility for ten irradiation-readout-annealing cycles.	101

4.11	Each data point is the average dose after ten repeated irradiation-readout-annealing cycles, with error bars representing their associated coefficient of variation.	102
4.12	Distribution of mean doses compared to the expected value (dotted line). Each data point corresponds to mean dose from the three nanoDots measured per cycle.	103
4.13	Comparison of dose linearity from nanoDots and TLD-100 chips to ion-chamber, with each data point for OSLD and TLD representing average dose of the three dosimeters.	104
4.14	PMT counts response with increasing absorbed dose. The corresponding counting errors decline with increasing absorbed dose.	105
4.15	(a) OSLD response determined as the ratio of measured to delivered dose, with error bars representing the standard deviation obtained from the three nanoDots used per data point. (b) OSLD response (count/dose normalized to minimum value) versus absorbed. The values of <i>a</i> , <i>b</i> , and <i>c</i> are 1.029, 0.011 and -4.049 respectively.	106
4.16	OSLD dose response when subjected to increasing mAs at fixed tube voltage.	108
4.17	Normalized counts versus measured dose depicting the linear response of the nanoDots at 80 kV, with corresponding counting errors.	109
4.18	Normalized counts versus measured dose depicting the linear response of the nanoDots at 120 kV, with corresponding counting errors.	110
4.19	Relative energy response of the OSLDs and TLDs irradiated under the same condition, where each data point represents the average response from three OSLDs and three TLDs.	111
4.20	OSLDs measured dose showing a significant variation compared to ion-chamber (reference detector). The error bars represent standard deviation of three readings of the three OSLDs used per exposure.	112
4.21	Schematic diagram showing the irradiation setup for angular dependence measurement using 80 kV beam and 8 mGy using Philips Industrial X-ray unit.	115
4.22	Angular dependence of nanoDot with 80 kVp X-ray beam normalized to dose at 90°. The error bars represent the standard deviation of the mean.	115

4.23	OSL signal depletion in 25 sequential readings for three dosimeters exposed to single dose of 20 mGy with all data normalized to the first reading.	116
4.24	Element correction factors of individual nanoDots when subjected to identical irradiation condition.	118
4.25	Trumpet curve displaying the ratio, $R$ , as a function of delivered dose $H_p(10)_{del}$ . The solid line ( $R_{UL}$ ) and dotted line ( $R_{LL}$ ) represent the upper and lower limits of the trumpet curve respectively.	120
4.26	Trumpet curve of dosimeters used for linearity and energy dependence. Each data point represents the ratio $R$ , of a single nanoDot. Doses used for linearity were 5, 8, 10, 15 and 20 mGy, while 8 mGy was used for energy dependence.	121
4.27	Mean ESD in each field size for the different projections.	124
4.28	Histogram showing the ESD distribution averaged across the selected field sizes per X-ray examination.	128
4.29	Chart of ESDs achieved by the present work compared with established international DRLs.	135
4.30	Comparison of measured ESDs with PA chest established DRLs.	142



## LIST OF ABBREVIATIONS

AAPM	-	American Association of Physicists in Medicine
Al <sub>2</sub> O <sub>3</sub> :C	-	Aluminium Oxide doped with Carbon
AP	-	Anterior Posterior
BMI	-	Body-Mass Index
BSF	-	Backscatter Factor
BSS	-	Basic Safety Standard
CBCT	-	Cone-Beam Computed Tomography
CF	-	Conversion Factor/Calibration Factor
CT	-	Computed Tomography
CW-OSL	-	Continuous Wave – Optically Stimulated Luminescence
CV	-	Coefficient of Variation
DRK	-	Dark Current
DRL	-	Diagnostic Reference Level
EC	-	European Commission
ECF	-	Energy Correction Factor/Element Correction Factor
ESAK	-	Entrance Surface Air Kerma
ESD	-	Entrance Surface Dose
EU	-	European Union
FDD	-	Focus to Detector Distance
FSD	-	Focus to Surface Distance
FTD	-	Focus to Table top Distance
GE	-	General Electric
HVL	-	Half Value Layer
IAEA	-	International Atomic Energy Agency
ICRP	-	International Commission on Radiation Protection
ICRU	-	International Commission on Radiation Units
IEC	-	International Electrotechnical Commission
IKN	-	Institute Kanser Negara
INAK	-	Incident Air Kerma
KV XVI	-	Kilo Voltage X-ray Volume Imager

LAT	-	Lateral
LED	-	Light Emitting Diode
LM-OSL	-	Linear Modulated – Optically Stimulated Luminescence
LNT	-	Linear No Threshold
MNA	-	Malaysian Nuclear Agency
MOSFET	-	Metal Oxide Semiconductor Field Effect Transistor
OSL	-	Optically Stimulated Luminescence
OSLD	-	OSL Dosimeter
PA	-	Posterior Anterior
PET	-	Positron Emission Tomography
PMT	-	Photo-Multiplier Tube
POSL	-	Pulsed-Optically Stimulated Luminescence
PSDL	-	Primary Standard Dosimetry Laboratory
PTB	-	Physikalisch-Technische Bundesanstalt
QA	-	Quality Assurance
QC	-	Quality Control
SD	-	Standard Deviation
SF	-	Sensitivity Factor
SSD	-	Source to Sample Distance
SSDL	-	Secondary Standard Dosimetry Laboratory
TL	-	Thermo-Luminescence
TLD	-	TL Dosimeter
UNSCEAR	-	United Nation Scientific Committee on Effects of Atomic Radiations

## LIST OF SYMBOLS

$I$	-	Final Intensity
$I_0$	-	Initial Intensity
$Z_{eff}$	-	Effective Atomic Number
$Z$	-	Atomic Number
$\mu$	-	Absorption Coefficient
$h\nu$	-	Photon Energy
$E$	-	Energy
$E_e$	-	Electron Energy
$E_b$	-	Electron Binding Energy
$\tau$	-	Photoelectric Cross-section
$N$	-	Number of Atoms per unit Volume
$\theta$	-	Angle
$mc^2$	-	Rest-mass Energy
$k$	-	Boltzmann's Constant
$T$	-	Temperature
$n$	-	Trapped Charge Concentration
$p$	-	Rate of Stimulation
$\Phi$	-	Photon Flux
$\sigma$	-	Photo-ionisation Cross-section
$\lambda$	-	Wavelength
$f(D)$	-	Dose Response Function
$D$	-	Absorbed Dose
$S(n)$	-	OSL signal on $n$ readings
$\bar{\varepsilon}$	-	Energy Imparted
$R_{in, out}$	-	Radiant energy
$Q$	-	Charge
$H_T$	-	Dose Equivalent
$w_R$	-	Weighing Factor
$K_i$	-	Incident Air Kerma
$K(d)$	-	Air Kerma at the Measurement Point

$d_{FTD}$	-	Distance between Tube Focus to Patient Support
$d_m$	-	Distance from table top to reference point
$t_p$	-	Patient's organ thickness
$K_e$	-	Entrance Air Kerma
$Y(d)$	-	Tube Output
$P_{It}$	-	Current-Exposure time product
$\rho$	-	Density
$\mu_{en}$	-	Mass-Energy Absorption Coefficient
$R_{uL}$	-	Upper Limit of measured to delivered dose ratio
$R_{LL}$	-	Lower Limit of measured to delivered dose ratio
$H_0$	-	Lowest Dose
$H_1$	-	Conventional True Dose

## LIST OF APPENDICES

<b>APPENDIX</b>	<b>TITLE</b>	<b>PAGE</b>
Appendix A	Some Important Formulae	162
Appendix B	Uncertainty Analysis	164
Appendix C	Table showing the data for $R_{UL}$ and $R_{LL}$ used in the trumpet curve	166
Appendix D	Example of raw data output from microStar reader	167

# CHAPTER 1

## INTRODUCTION

### 1.1 Background of the Research

The use of optically stimulated luminescence (OSL) technique for a variety of radiation dosimetry applications in recent years is increasing due to the dramatic growth in the use of ionizing radiation for clinical purpose. Since the inception of OSL technique for dosimetry applications in the 80s, a good number of studies have been carried out to comprehend the luminescence properties of different materials (Huntley, Godfrey-Smith and Thewalt, 1985). The most essential factors that define a successful measurement in radiation dosimetry are traceability, consistency and accuracy, particularly in radiology and radiotherapy where the outcome is highly dependent on the radiation dose delivered to the patient (IAEA, 2009). The need for radiological techniques such as general radiography and computed tomography (CT) for diagnostic purposes has increased significantly in the last few decades which resulted to high demand of radiation monitoring mechanisms to assess the risk-to-benefit relationship associated with the use of these modalities and to keep the dose levels of patients and personnel as low as reasonably achievable (ALARA) in order to avoid the risk of cancer induction associated with diagnostic radiations.

Estimation of doses in diagnostic radiology is usually done by entrenching a dosimeter in the patient's/personnel's body or tissue-equivalent phantom. Both thermoluminescence dosimeter (TLD) and OSLD are known to be utilized for radiation dosimetry including personal monitoring, in-vivo dosimetry and estimation of dose index in computed tomography (CT) from the dose profiles (Endo *et al.*, 2012). The application of optically stimulated luminescence (OSL) technique is not limited to personal and medical dosimetry, but has recently been used for the assessment of environmental dose using naturally occurring minerals in luminescence dating and

retrospective dosimetry which serve as leap forward in the development of OSL readers (Yukihara and McKeever, 2008).

The use of X-rays in diagnostic radiology has contributed immensely to the identification and treatment of countless number of diseases and helps to improve the health of people, but at the same time, radiation doses from diagnostic radiology have the largest contributions to the combined dose from all artificial sources of radiation which is attributed to the large number of X-ray examinations performed annually (IAEA, 2007). According to the recent analysis by United Nations Scientific Committee on the Effects of Atomic Radiation (UNSCEAR), an estimated 3.6 billion diagnostic X-ray examinations are undertaken annually worldwide (UNSCEAR, 2011). This shows that there is high increase of patient exposure to ionizing radiation in order to provide a proper diagnosis at the same time using high exposure to produce images of good quality. Therefore, dosimetric technique is required in diagnostic X-ray imaging systems in order to determine the dosimetric parameters for establishing diagnostic reference levels (DRL) and assessing the average dose to the tissues and organs at risk.

Any exposure to ionising radiation is presumed to give rise to a risk of detrimental effects, such that one has to recognize that there is certain degree of risk involved and must limit the radiation dose to a level at which the assumed risk is considered to be acceptable or permissible in view of the benefits derived from such procedures (ICRP, 1977). Part of the European Union recommendation for efficient radiation protection was to reduce unproductive and needless radiation exposure by optimization of protection measures and use of dose limits (European Commission, 1999). This is because despite the net benefit in these procedures supersede the risk, the potential for radiation-induced injuries to patient remain possible.

Assessment of dose and determination of dosimetric parameters would not be possible without evaluating the associated dosimetry equipment performance as part of the requirement and quality assurance process (IAEA, 2007). It is therefore necessary and essential to test the performance of new dosimetry equipment for quality control and assurance. Entrance surface dose (ESD) is an important parameter in

assessing the dose delivered to patient in a single radiographic exposure. The European Union (EU) has identified this physical quantity as one to be monitored as a diagnostic reference level (DRL) which permits optimization of patient dose. Patient doses in diagnostic X-ray examinations can be best estimated in terms of the entrance surface dose (ESD) per radiograph or dose area product (DAP) for the complete examination (European Commission, 1996). However, TLD is the most widely used dosimeter for ESD measurement in clinical dosimetry but the prevailing potentials of OSLD to be used for nearly real time dosimetry has given OSL a good level of superiority in some aspects (McKeever and Moscovitch, 2003). Monte Carlo simulations of the energy deposition from X-ray exposure can also be achieved, provided the irradiation conditions related to the X-ray procedure and anatomy of the patient under study are well defined (Meghzifene *et al.*, 2010). By means of dosimeter or ionization chamber, ESD can also be measured directly with the use of suitable phantoms (Ng and Yeong, 2014).

The availability of commercial OSL dosimeters has also contributed to the successful applications of OSL technique for clinical and personal use. The InLight and nanoDots OSL dosimeters made of up  $\text{Al}_2\text{O}_3:\text{C}$  produced by Landauer had extensively been used for dosimetry applications in recent years (Yukihara and McKeever, 2008). But the use of this dosimetry system is not rapidly migrating into diagnostic radiology especially radiography, with majority of the recent studies giving emphasis to image quality and overlooking the possible risk of radiation exposure to patients.

## **1.2 Problem Statements**

In a properly managed diagnostic X-ray examinations, the radiation doses which typically range from 1 – 20 mGy are far much lower than those capable of producing noticeable serious radiation injury (IAEA, 2007). Yet, there may be no such lower dose limit for the instigation of some deleterious effects (stochastic effects). Such small doses may give rise to malignant neoplasia and radiation-induced mutation, which in turn may form the basis of hereditary effects. Thus, the possible risk from



small doses due to exposure to ionizing radiation is perhaps owing to these types of biological changes and any increment of doses to individuals from X-ray carries certain amount of risk, even though the risk may be extremely small. According Linear No Threshold (LNT) hypothesis, any dose, whatever small, can produce a detriment and the risk excess of developing a radiation-induced disease increases with the dose to the individual linearly (Ferdegini, 2014). However, the appropriate action that should be taken to prevent unnecessary exposure in radiography is to regularly monitor the radiation dose used for each procedure using a suitable technique by trained staff (IAEA, 2007).

This has attracted a lot of research interest to the use of OSL dosimeters as potential alternative to the well-known TLDs. TLDs are highly sensitive devices and have been used extensively on patients as well as on phantoms. But the destructive readout feature of the TLD limits the reanalysis of the absorbed dose. (McKeever and Moscovitch, 2003; Meigooni *et al.*, 1995; Olko, 2010). Measurement using ionization chambers can also be made with high degree of accuracy than other dosimeters, but require sophisticated electrometer circuit and storage facility, and are not always used on patients due to their bulkiness and connecting cables that inconvenience the patient mobility with potential interfering shadow on the radiograph (Merchant, 1933; Massoud E, 2014; Ponmalar *et al.*, 2017). Despite good reproducibility and real-time readout of the Metal Oxide Semiconductor Field Effect Transistor (MOSFET) based dosimeter, the presence of finite lifetime and temperature dependence limit their application (Ponmalar *et al.*, 2017; Rahman *et al.*, 2016; Rivera-Montalvo, 2016).

Owing to their excellent dosimetric attributes, the aluminium oxide based ( $\text{Al}_2\text{O}_3:\text{C}$ ) OSL dosimeter developed by Landauer Inc, have been used extensively in clinical radiotherapy (Mrčela *et al.*, 2011; Andersen, Aznar and Boetter-Jensen, 2003; Dunn *et al.*, 2013; Jursinic, 2007; Jursinic, 2010; Ponmalar *et al.*, 2017; Viamonte *et al.*, 2008), and diagnostic radiology procedures including computed tomography (CT) (Al-Senan and Hatab, 2011; Ding and Malcolm, 2013; Scarboro *et al.*, 2015; Tawfik *et al.*, 2013; Yukihiro *et al.*, 2009; Yusuf *et al.*, 2014), fluoroscopy (Akselrod, Botter-Jensen and McKeever, 2006; Gasparian *et al.*, 2010; Perks, Yahnke and Million, 2008), and mammography (Al-Senan and Hatab, 2011; Alothmany *et al.*, 2016; Perks,

Yahnke and Million, 2008). In spite of the interesting features of the Al<sub>2</sub>O<sub>3</sub>:C OSLDs in radiation dosimetry, which include high sensitivity, good precision for low dose measurements, possible re-analysis, high speed readout and elimination of thermal annealing steps (McKeever and Moscovitch, 2003; Olko, 2010), all-inclusive literature review revealed that the use of Al<sub>2</sub>O<sub>3</sub>:C OSLDs in general X-ray is not well-established. This is attributed to the fact the material over-respond to low energy X-rays about 3 – 4 times at an effective energy of ~40 – 50 keV compared to higher energy photons from <sup>60</sup>Co or <sup>137</sup>Cs due to its high effective atomic number (11.28), resulting to certain level of energy dependence (Yukihara *et al.*, 2009).

The principal goal of this research is to characterize the nanoDot OSLDs in radiography energy range (40 – 150 kV), with the aim of providing solutions involving over-response and energy dependence associated to the Al<sub>2</sub>O<sub>3</sub> material in low energy X-ray, and to assess the suitability of the nanoDot OSLDs for entrance surface dose (ESD) assessment in diagnostic X-ray examinations. The major significance and relevance of this research is to offer an alternative for ESD determination using OSL through provision of new data for common X-ray examinations and relevant dosimetric characteristics. The problem statement of the study is shown schematically in Figure 1.1.

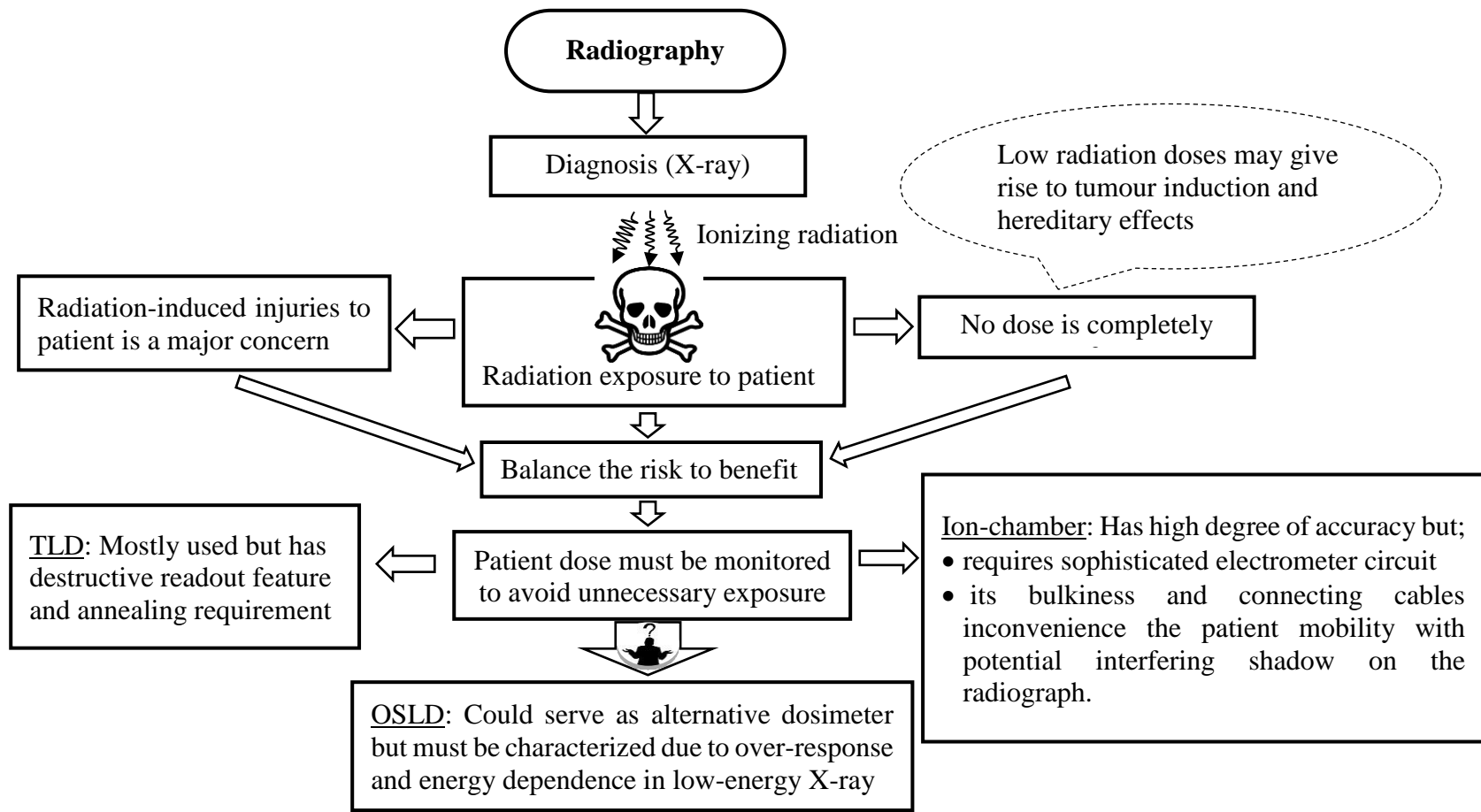


**Figure 1.1** Schematic diagram of the research problem statement.

### **1.3 Aim and Objectives of the Research**

This study is aimed to characterize the new OSL dosimetry system in UTM supplied by Landauer Inc and evaluate its suitability for clinical dosimetry in general X-ray. The objectives of this research are as follows;

- (a) To calibrate and evaluate the stability of the new Landauer InLight MicroStar OSL dosimetry system.
- (b) To investigate the dosimetric characteristics of the nanoDots OSLD including repeatability, reproducibility, dose linearity, signal depletion, element correction factor, angular dependence, and energy dependence in radiography energy range from 40 kV – 150 kV with typical doses ranging from 0 – 20 mGy.
- (c) To assess the suitability of the nanoDots OSLD for direct and indirect ESD measurements in Chest, Abdomen, Skull, and Thoracic spine radiography, with associated eye, thyroid and gonad doses using adult anthropomorphic phantom and compare with CALDose\_X 5.0 software calculations.

### **1.4 Scope of the Research**

The current study involves the evaluation of the InLight microStar reader performance, characterization of the OSL dosimeters and their applications for ESD measurement in common X-ray examinations. The scope of this study is itemized as follows;

The baseline of the OSL reader performance was established by assessing the reader stability based on background signal fluctuations. Afterwards, the microStar reader was calibrated using OSL dosimeters irradiated to 80 kV X-ray beam and dose levels of 0 – 30 mGy for low dose calibration and 0 – 1000 mGy for high dose calibration.

The nanoDot OSLDs dosimetric characteristics were evaluated in radiation qualities for radiography (RQR) by assessing the repeatability, reproducibility, signal depletion, dose-response linearity, individual dosimeter element correction factors, energy dependence, angular dependence and dose measurements accuracy in the energy range from 40 – 150 kV using typical doses in radiography ranging from 0 -20 mGy.

Entrance surface doses (ESDs) were measured using the so-called *Indirect measurement* and *Direct measurement* methods based on the IAEA procedures described in Technical Report Series No. 457. Direct measurements were performed using anthropomorphic whole-body phantom, while indirect measurements were performed in the absence of backscatter material. The common X-ray examinations that were considered are: AP abdomen, LAT abdomen, AP chest, PA chest, AP thoracic spine and AP skull.

Mathematical software known as CALDose\_X 5.0 was utilized to calculate ESDs in the X-ray examinations mentioned earlier, using the same exposure parameters as employed in the measurement methods. The measured ESDs were then validated by comparison with CALDose\_X software calculations, published works and established international diagnostic reference levels (DRLs).

Doses to the critical organs such as eye, thyroid and gonad were also measured using direct method during the AP abdomen, AP chest and AP skull examinations.

## **1.5 Thesis Outline**

This thesis is designed to give a broad overview of the use of optically stimulated luminescence dosimetry for entrance surface dose measurements in radiography. The steps taken for achieving this goal was exclusively experimental, which involved understanding the basic technique required for ESD estimation in common X-ray examinations.

## REFERENCES

- AAPM (1990). *Standardized methods for measuring diagnostic X-ray exposures. AAPM Report No. 31*, New York, NY.
- Akselrod, M.S., Botter-Jensen, L. and McKeever, S.W.S. (2006). Optically stimulated luminescence and its use in medical dosimetry. *Radiation Measurements*. 41(1), S78–S99.
- Akselrod, M.S., Kortov, V.S., Kravetsky, D.J. and Gotlib, V.I. (1990). Highly sensitive thermoluminescent anion-defective alpha-Al<sub>2</sub>O<sub>3</sub>:C single crystal detectors. *Radiation Protection Dosimetry*. 32(1), 15–20.
- Al-Senan, R.M. and Hatab, M.R. (2011). Characteristics of an OSLD in the diagnostic energy range. *Medical Physics*. 38(7), 4396–4405.
- Almen, A., Bernhardt, J., Johansson, L., Kasch, K., Kaul, A., Kramer, H., Mattsson, S., Moores, B., Nobke, D., Selbach, H., Stieve, F., Valentine, J. and Vatnitsky, S. (2012). *Medical radiological physics* A. Kaul, ed., Berlin, Heidelberg: Springer.
- Alothmany, N., Molla, N.I., Yusuf, M., Hussain, A., Mail, N., Alothmany, D., Khafaji, M.A., Natto, H., Tayeb, M., Nadwi, F., Jiman, A. and Kinsara, A.A. (2016). Characterization of optically stimulated luminescence for assessment of breast doses in mammography screening. *Radioprotection*. 51(1), 51–58.
- Andersen, C.E., Aznar, M.C. and Boetter-Jensen, L. (2003). Development of optical fibre luminescence techniques for real time in vivo dosimetry in radiotherapy. In *Standard code of practice in medical radiation dosimetry, international symposium (IAEA-CN-96/118), Vienna, IAEA*. pp.353–360.
- Andersen, C.E., Nielsen, S.K., Greilich, S., Helt-Hansen, J., Lindegaard, J.C. and Tanderup, K. (2009). Characterization of a fiber-coupled Al<sub>2</sub>O<sub>3</sub>:C luminescence dosimetry system for online in vivo dose verification during <sup>192</sup>Ir brachytherapy. *Medical Physics*. 36(3), 708–718.
- Antonov-Romanovskii, V. V, Kcium-Marcus, I.F., Poroshina, M.S. and Trapeznikova, A.Z. (1956). USAEC Report AEC-tr-2435. In *Conference of the Academy of Sciences of the USSR on the peaceful uses of Atomic Energy, Moscow, 1955. USAEC Report AEC-tr-2435*.

- Arib, M., Herrati, A., Dari, F., Ma, J. and Lounis-Mokrani, Z. (2014). Intercomparison 2013 on measurements of the personal dose equivalent  $H_p(10)$  in photon fields in the African region. *Radiation Protection Dosimetry*. 163(3), 276–283.
- Aznar, M.C., Andersen, C.E., Bøtter-Jensen, L., Bäck, S.Å.J., Mattsson, S., Kjær-Kristoffersen, F. and Medin, J. (2004). Real-time optical-fibre luminescence dosimetry for radiotherapy: physical characteristics and applications in photon beams. *Physics in Medicine and Biology*. 49(9), 1655–1669.
- Beyzadeoglu, M., Ozyigit, G. and Ebruli, C. (2010). *Basic radiation oncology*, Springer-Verlag.
- Bickle, I. and Morgan, M.A. (2018). Abdomen ( lateral decubitus view ). *Radiopaedia*., 1–8. Available at: <https://radiopaedia.org/articles/abdomen-lateral-decubitus-view-1>.
- Boetter-Jensen, L., McKeever, S.W.. and Wintle, A.G. (2003). *Optically stimulated luminescence dosimetry* 1st ed., Amsterdam: Elsevier.
- Bøtter-Jensen, L., Banerjee, D., Jungner, H. and Murray, A.S. (1999). Retrospective assessment of environmental dose rates using optically stimulated luminescence from  $Al_2O_3:C$  and quartz. In *Radiation Protection Dosimetry*. pp.537–542.
- Bøtter-Jensen, L., McKeever, S.W.S. and Wintle, A.G. (2003). *Optically stimulated luminescence dosimetry* 1st editio., Amsterdam: Elsevier.
- Brant, E.W. and Clyde, A.H. (2007). *Fundamentals of diagnostic radiology* 3rd ed. W. E. Brant & C. A. Helms, eds., Lippincott Williams & Wilkins.
- Brennan, P.C., McDonnell, S. and O’Leary, D. (2004). Increasing film-focus distance (FFD) reduces radiation dose for x-ray examinations. *Radiation Protection Dosimetry*. 108(3), 263–268.
- Bulur, E. (1996). An alternative technique for optically stimulated luminescence (OSL) experiment. *Radiation Measurements*. 26(5), 701–709.
- Bulur, E., Bøtter-jensen, L. and Murray, A.S. (2000). Optically stimulated luminescence from quartz measured using the linear modulation technique. *Radiation Measurements*. 32, 407–411.
- Camargo-Mendoza, R.E., Poletti, M.E., Costa, A.M. and Caldas, L.V.E. (2011). Measurement of some dosimetric parameters for two mammography systems using thermoluminescent dosimetry. *Radiation Measurements*. 46(12), 2086–2089.

- Chang, D.S., Lasley, F.D., Das, I.J., Mendonca, M.S. and Dynlacht, J.R. (2014). *Basic Radiotherapy Physics and Biology*, New York, NY: Springer.
- Compagnone, G., Pagan, L. and Bergamini, C. (2005). Comparison of six phantoms for entrance skin dose evaluation in 11 standard X-ray examinations. *Journal of Applied Clinical Medical Physics*. 6(1), 101–113.
- Costa, A.M. and Pelegrino, M.S. (2014). Evaluation of entrance surface air kerma from exposure index in computed radiography. *Radiation Physics and Chemistry*. 104, 198–200.
- Danzer, J., Dudney, C., Seibert, R., Robison, B., Harris, C. and Ramsey, C. (2007). TH-C-M100E-02: Optically Stimulated Luminescence of Aluminum Oxide Detectors for Radiation Therapy Quality Assurance. *Medical Physics*. 34(6), 2628-2629.
- DeWerd, L.A. and Lawless, M. (2014). Introduction to Phantoms of Medical and Health Physics. In *The Phantoms of Medical and Health Physics*. Springer New York, pp.1–14.
- Ding, G.X. and Malcolm, A.W. (2013). An optically stimulated luminescence dosimeter for measuring patient exposure from imaging guidance procedures. *Physics in Medicine and Biology*. 58(17), 5885–97.
- Dong, F., Davros, W., Pozzuto, J. and Reid, J. (2012). Optimization of kilovoltage and tube current-exposure time product based on abdominal circumference: An oval phantom study for pediatric abdominal CT. *American Journal of Roentgenology*. 199(3), 670–676.
- Dunn, L., Lye, J., Kenny, J., Lehmann, J., Williams, I. and Kron, T. (2013). Commissioning of optically stimulated luminescence dosimeters for use in radiotherapy. *Radiation Measurements*. 51–52, 31–39.
- Endo, A., Katoh, T., Kobayashi, I., Joshi, R., Sur, J. and Okano, T. (2012). Characterization of optically stimulated luminescence dosimeters to measure organ doses in diagnostic radiology. *Dentomaxillofacial Radiology*. 41(3), 211–216.
- European Commission (2014). Diagnostic Reference Levels in Thirty-six European Countries. Part 2/2. *Radiation Protection N° 180*.
- European Commission (1996). European Guidelines on Quality Criteria for Diagnostic Radiographic Images. *Eur 16260 En*.



- European Commission (1999). Guidance on diagnostic reference levels (DRLs) for medical exposures. *Radiation Protection 109*.
- Ferdeghini, E.M. (2014). *Radiation Protection and Dosimetry in x-Ray Imaging*, Elsevier B.V.
- Fung, K.K.L. and Gilboy, W.B. (2001). The effect of beam tube potential variation on gonad dose to patients during chest radiography investigated using high sensitivity LiF: Mg, Cu, P thermoluminescent dosimeters. *The British Journal of Radiology*. 74(880), 358–367.
- Gasparian, P.B.R., Ruan, C., Ahmad, S., Kalavagunta, C., Cheng, C.Y. and Yukihara, E.G. (2010). Demonstrating the use of optically stimulated luminescence dosimeters (OSLDs) for measurement of staff radiation exposure in interventional fluoroscopy and helmet output factors in radiosurgery. *Radiation Measurements*. 45(3–6), 677–680.
- Grondin, Y., Matthews, K., McEntee, M., Rainford, L., Casey, M., Tonra, M., Al-Qattan, E., McCrudden, T., Foley, M. and Brennan, P.C. (2004). Dose-reducing strategies in combination offers substantial potential benefits to females requiring X-ray examination. *Radiation Protection Dosimetry*. 108(2), 123–132.
- Grosswendt, B. (1984). Backscatter factors for x-rays generated at voltages between 10 and 100 kV. *Physics in Medicine and Biology*. 29(5), 579–591.
- Grosswendt, B. (1993). Dependence of the photon backscatter factor for water on irradiation field size and source-to-phantom distances between 1.5 and 10 cm. *Physics in Medicine and Biology*. 38(2), 305–310.
- Grosswendt, B. (1990). Dependence of the photon backscatter factor for water on source-to-phantom distance and irradiation field size. *Physics in Medicine and Biology*. 35(9), 1233–1245.
- Guimarães, C.C. and Okuno, E. (2003). Blind performance testing of personal and environmental dosimeters based on TLD-100 and natural CaF<sub>2</sub>:NaCl. *Radiation Measurements*. 37(2), 127–132.
- Habibzadeh, M.A., Ay, M.R., Asl, A.R.K., Ghadiri, H. and Zaidi, H. (2012). Impact of miscentering on patient dose and image noise in x-ray CT imaging: phantom and clinical studies. *Physica Medica*. 28(3), 191–199.
- Hart, D., Hillier, M.C. and Shrimpton, P.C. (2012). *HPA-CRCE-034 - Doses to Patients from Radiographic and Fluoroscopic X-ray Imaging Procedures in the UK – 2010 Review*,

- Hayashi, H., Takegami, K., Okino, H., Nakagawa, K., Okazaki, T. and Kobayashi, I. (2015). Procedure to measure angular dependences of personal dosimeters by means of diagnostic X-ray equipment. *Medical Imaging and Information Sciences*. 32(1), 8–14.
- Huntley, D.J., Godfrey-Smith, D.I. and Thewalt, M.L.W. (1985). Optical dating of sediments. *Nature*. 313(5998), 105–107.
- IAEA (1999). Assessment of occupational exposure due to external sources of radiation. *IAEA Safety Standards Series*. No. RS-G-1.
- IAEA (2009). Calibration of Reference Dosimeters for External Beam Radiotherapy. *Technical Reports Series No. 469*. (469).
- IAEA (2007). *Dosimetry in diagnostic radiology: an international code of practice TRS 457*, Vienna: IAEA.
- IAEA (2004). Optimization of the radiological protection of patients undergoing radiography, fluoroscopy and computed tomography. *IAEA-TECDOC-1423*.
- IAEA (2005). *Radiation Oncology Physics: A Handbook for Teachers and Students* E. B. Podgorsak, ed., IAEA.
- IAEA (2002). Radiological Protection for Medical Exposure to Ionizing Radiation. *IAEA Safety Standards Series No. RS-G-1.5*. PUB 1117.
- ICRP (1992). ICRP Publication 60: 1990 Recommendations of the international commission on radiological protection. *Annals of the ICRP*, 21 (1-3), 1991. *Annals of Nuclear Energy*. 19(1), 51–52.
- ICRP (1969). Protection of the Patient in X-ray Diagnosis. *ICRP Publication 16*.
- ICRP (1977). Recommendations of the International Commission on Radiological Protection. *ICRP Publication 26*.
- Ikmal, W.N.S.W., Samat, S.B. and Kadir, A.B.A. (2016). Evaluation of deep and shallow doses for OSLD and TLD-100H. In *AIP Conference Proceedings*. p.040023.
- Jennings, W.A. (1994). Quantities and units in radiation protection dosimetry. *Nuclear Inst. and Methods in Physics Research, A*. 346(3), 548–549.
- Jibiri, N.N. and Olowookere, C.J. (2016). Patient dose audit of the most frequent radiographic examinations and the proposed local diagnostic reference levels in southwestern Nigeria: Imperative for dose optimisation. *Journal of Radiation Research and Applied Sciences*. 9(3), 274–281.

- Jursinic, P.A. (2010). Changes in optically stimulated luminescent dosimeter (OSLD) dosimetric characteristics with accumulated dose. *Medical physics*. 37(1), 132–40.
- Jursinic, P.A. (2007). Characterization of optically stimulated luminescent dosimeters, OSLDs, for clinical dosimetric measurements. *Medical Physics*. 34(12), 4594–4604.
- Karami, V., Zabihzadeh, M., Danyaei, A. and Shams, N. (2016). Efficacy of Increasing Focus to Film Distance (FFD) for Patient’s Dose and Image Quality in Pediatric Chest Radiography. *Int J Pediatr*. 4(9), 3421–3429.
- Kawaguchi, A., Matsunaga, Y., Suzuki, S. and Chida, K. (2017). Energy dependence and angular dependence of an optically stimulated luminescence dosimeter in the mammography energy range. *Journal of Applied Clinical Medical Physics*. 18(2), 191–196.
- Kerns, J.R., Kry, S.F., Sahoo, N., Followill, D.S. and Ibbott, G.S. (2011). Angular dependence of the nanoDot OSL dosimeter. *Medical Physics*. 38(7), 3955–62.
- Klein, D.M., Yukihara, E.G., McKeever, S.W.S., Durham, J.S. and Akselrod, M.S. (2006). In situ long-term monitoring system for radioactive contaminants. *Radiation Protection Dosimetry*. 119(1–4), 421–424.
- Klevenhagen, S.C. (1989). Experimentally determined backscatter factors for X-rays generated at voltages between 16 and 140 kV. *Physics in Medicine and Biology*. 34(12), 1871–1882.
- Klevenhagen, S.C. (1982). The build-up of backscatter in the energy range 1 mm Al to 8 mm Al HVT (radiotherapy beams). *Physics in Medicine and Biology*. 27(8), 1035–1043.
- Klevenhagen, S.C., Aukett, R.J., Harrison, R.M., Moretti, C., Nahum, A.E. and Rosser, K.E. (1996). The IPEMB code of practice for the determination of absorbed dose for X-rays below 300 kV generating potential (0.035 mm Al–4 mm Cu HVL; 10 - 300 kV generating potential). *Physics in Medicine and Biology*. 41, 2605–2625.
- Kramer, R., Khoury, H.J. and Vieira, J.W. (2008). CALDose X—a software tool for the assessment of organ and tissue absorbed doses, effective dose and cancer risks in diagnostic radiology. *Physics in Medicine and Biology*. 53, 6437–6459.
- Landauer (2012). *InLight microStar system user manual* Version 4., Landauer Inc.
- Landauer (2015). nanoDot and microSTARii: Frequently Asked Questions. [http://www.landauer.com/uploadedFiles/About\\_Us/microSTARii\\_FAQ.pdf](http://www.landauer.com/uploadedFiles/About_Us/microSTARii_FAQ.pdf).

- Lim, C.S., Lee, S.B. and Jin, G.H. (2011). Performance of optically stimulated luminescence  $\text{Al}_2\text{O}_3$  dosimeter for low doses of diagnostic energy X-rays. *Applied Radiation and Isotopes*. 69(10), 1486–1489.
- Malaysia, M. of H. (2013). Malaysian diagnostic reference levels in medical imaging (Radiology). *Radiation Health and Safety Section Engineering Services Division, Ministry of Health Malaysia*.
- Manji, F., Wang, J., Norman, G., Wang, Z. and Koff, D. (2016). Comparison of dual energy subtraction chest radiography and traditional chest X-rays in the detection of pulmonary nodules. *Quantitative imaging in medicine and surgery*. 6(1), 1–5.
- Manning-Stanley, A.S., Ward, A.J. and England, A. (2012). Options for radiation dose optimisation in pelvic digital radiography: A phantom study. *Radiography*. 18(4), 256–263.
- Massoud E, D.H. (2014). Optimization of Dose to Patient in Diagnostic Radiology Using Monte Carlo Method. *Journal of Cell Science & Therapy*. 05(01), 1–6.
- McKeever, S.W.S. (1988). *Thermoluminescence of Solids*, New York: Cambridge University Press.
- McKeever, S.W.S., Akselrod, M. and Markey, B.G. (1996). Pulsed Optically Stimulated Luminescence Dosimetry Using Alpha- $\text{Al}_2\text{O}_3\text{:C}$ . *Radiation Protection Dosimetry*. 65(1), 267–272.
- McKeever, S.W.S. and Moscovitch, M. (2003). On the advantages and disadvantages of optically stimulated luminescence dosimetry and thermoluminescence dosimetry. *Radiation Protection Dosimetry*. 104(3), 263–270.
- Meghzifene, A., Dance, D.R., McLean, D. and Kramer, H.M. (2010). Dosimetry in diagnostic radiology. *European Journal of Radiology*. 76(1), 11–14.
- Meigooni, A.S., Mishra, V., Panth, H. and Williamson, J. (1995). Instrumentation and dosimeter-size artifacts in quantitative thermoluminescence dosimetry of low-dose fields. *Medical Physics*. 22(5), 555–561.
- Merchant, A.K. (1933). The Advantages and Disadvantages of Large Chamber Measuring Apparatus 1. *Radiology*. 21(2), 123–125.
- Mery, D. (2015). *Computer Vision for X-Ray Testing: Imaging, Systems, Image Databases, and Algorithms*, Springer.
- Mobit, P., Agyingi, E. and Sandison, G. (2006). Comparison of the energy-response factor of  $\text{LiF}$  and  $\text{Al}_2\text{O}_3$  in radiotherapy beams. *Radiation Protection Dosimetry*. 119(1–4), 497–499.

- Mrčela, I., Bokulić, T., Izewska, J., Budanec, M., Fröbe, A. and Kusić, Z. (2011). Optically stimulated luminescence in vivo dosimetry for radiotherapy: physical characterization and clinical measurements in  $^{60}\text{Co}$  beams. *Physics in Medicine and Biology*. 56(18), 6065–6082.
- Muhogora, W.E. and Nyanda, A.M. (2001). Experiences with the European guidelines on quality criteria for radiographic images in Tanzania. *Journal of Applied Clinical Medical Physics*. 2(4), 219–226.
- NCRP (1993). Exposure of the U.S population from diagnostic medical radiation. *NCRP report No. 100*.
- Ng, K.-H. and Yeong, C.-H. (2014). Imaging Phantoms: Conventional X-ray Imaging Applications. In L. A. DeWerd & M. Kissick, eds. *The Phantoms of Medical and Health Physics*. Springer New York, pp.91–122.
- Ng, K., Rassiah, P., Wang, H., Hambali, A.S., Muthuvellu, P. and Lee, H. (1998). Doses to patients in routine X-ray examinations in Malaysia. *The British Journal of Radiology*. 71, 654–660.
- NRPB (1992). National protocol for patient dose measurements in diagnostic radiology. *Dosimetry Working Party of the Institute of Physical Sciences in Medicine*.
- Obed, R.I., Ademola, A., Adewoyin, K. and Okunade, O. (2007). Doses to patients in routine X-ray examinations of chest, skull, abdomen and pelvis in nine selected hospitals in Nigeria. *Research Journal of Medical Sciences*. 1(4), 209–214.
- Ofori, K., Gordon, S.W., Akrobortu, E., Ampene, A.A. and Darko, E.O. (2014). Estimation of adult patient doses for selected X-ray diagnostic examinations. *Journal of Radiation Research and Applied Sciences*. 7(4), 459–462.
- Okazaki, T., Ha yashi, H., Takegami, K., Okino, H., Kimoto, N., Maehata, I. and Kobayashi, I. (2016). Fundamental Study of nanoDot OSL Dosimeters for Entrance Skin Dose Measurement in Diagnostic X-ray Examinations. *Journal of Radiation Protection and Research*. 41(3), 229–236.
- Olko, P. (2010). Advantages and disadvantages of luminescence dosimetry. *Radiation Measurements*. 45(3–6), 506–511.
- Omrane, L. Ben, Verhaegen, F., Chahed, N. and Mtimet, S. (2003). An investigation of entrance surface dose calculations for diagnostic radiology using Monte Carlo simulations and radiotherapy dosimetry formalisms. *Physics in Medicine and Biology*. 48(12), 1809–1824.

- Parry, R.A., Glaze, S.A. and Archer, B.R. (1999). The AAPM/RSNA Physics Tutorial for Residents: Typical patient radiation doses in diagnostic radiology. *RadioGraphics*. 19(5), 1289–1302.
- Perks, C.A., Le Roy, G. and Prugnaud, B. (2007). Introduction of the InLight monitoring service. In *Radiation Protection Dosimetry*. pp.220–223.
- Perks, C.A., Yahnke, C. and Million, M. (2008). Medical dosimetry using Optically Stimulated Luminescence dots and microStar® readers. *12th International Contress of the International Radiation Protection Association.*, 10.
- Physikalisch-Technische Bundesanstalt (2015). Radiation qualities used in general radiography and fluoroscopy.  
[https://www.ptb.de/cms/fileadmin/internet/fachabteilungen/abteilung\\_6/6.2/6.25/ptb\\_rad\\_qual\\_2015\\_01\\_07.pdf](https://www.ptb.de/cms/fileadmin/internet/fachabteilungen/abteilung_6/6.2/6.25/ptb_rad_qual_2015_01_07.pdf), 1–8.
- Pina, D.R., Duarte, S.B., Netto, T.G., Trad, C.S., Brochi, M.A.C. and Oliveira, S.C. de (2004). Optimization of standard patient radiographic images for chest, skull and pelvis exams in conventional x-ray equipment. *Physics in Medicine and Biology*. 49(14), N215–N226.
- Pinto, T.N.O., Cecatti, S.G.P., Gronchi, C.C. and Caldas, L.V.E. (2008). Application of the OSL technique for beta dosimetry. *Radiation Measurements*. 43(2–6), 332–334.
- Ponmalar, R., Manickam, R., Ganesh, K., Saminathan, S., Raman, A. and Godson, H. (2017). Dosimetric characterization of optically stimulated luminescence dosimeter with therapeutic photon beams for use in clinical radiotherapy measurements. *Journal of Cancer Research and Therapeutics*. 13(2), 304.
- Pradhan, A.S., Lee, J.I. and Kim, J.L. (2008). Recent developments of optically stimulated luminescence materials and techniques for radiation dosimetry and clinical applications. *Journal of Medical Physics*. 33(3), 85–99.
- Rahman, A.K.M.M., Zubair, H.T., Begum, M., Abdul-Rashid, H.A., Yusoff, Z., Omar, N.Y.M., Ung, N.M., Mat-Sharif, K.A. and Bradley, D.A. (2016). Real-time dosimetry in radiotherapy using tailored optical fibers. *Radiation Physics and Chemistry*. 122, 43–47.
- Rasuli, B., Ghorbani, M. and Juybari, R.T. (2016). Radiation dose measurement for patients undergoing common spine medical x-ray examinations and proposed local diagnostic reference levels. *Radiation Measurements*. 87, 29–34.

- Rebuffel, V. and Dinten, J. (2007). Dual-Energy X-Ray Imaging : Benefits and Limits. *Insight-non-destructive Testing and Condition*. 49(10), 589–594.
- Reft, C.S. (2009). The energy dependence and dose response of a commercial optically stimulated luminescent detector for kilovoltage photon, megavoltage photon, and electron, proton, and carbon beams. *Medical Physics*. 36(5), 1690–1699.
- Reid, J., Gamberoni, J., Dong, F. and Davros, W. (2010). Optimization of kVp and mAs for pediatric low-dose simulated abdominal CT: Is it best to base parameter selection on object circumference? *American Journal of Roentgenology*. 195(4), 1015–1020.
- Rejab, M., Wong, J.H.D., Jamalludin, Z., Jong, W.L., Malik, R.A., Wan Ishak, W.Z. and Ung, N.M. (2018). Dosimetric characterisation of the optically-stimulated luminescence dosimeter in cobalt-60 high dose rate brachytherapy system. *Australasian Physical & Engineering Sciences in Medicine*. 41(2), 475–485.
- Rivera-Montalvo, T. (2016). Diagnostic radiology dosimetry: Status and trends. *Applied Radiation and Isotopes*. 117, 74–81.
- Ronda, C.R. (2008). *Luminescence: From Theory to Applications*, John Wiley & Sons.
- Saeed, M.K. (2015). Regional survey of entrance surface dose to patients from X-ray examinations in Saudi Arabia. *Australasian Physical & Engineering Sciences in Medicine*. 38(2), 299–303.
- Scarboro, S.B., Cody, D., Alvarez, P., Followill, D., Court, L., Stingo, F.C., Zhang, D., McNitt-Gray, M. and Kry, S.F. (2015). Characterization of the nanoDot OSLD dosimeter in CT. *Medical Physics*. 42(4), 1797–1807.
- Schulman, J.H. (1959). Solid state dosimeters for radiation measurement. In *No. A/Conf 15/P/1859. Naval Research Lab., Washington, DC*.
- Sharma, S.D., Sharma, R., Mulchandani, U., Chabey, A., Chourasia, G. and Mayya, Y.S. (2013). Measurement of entrance skin dose for diagnostic x-ray radiographic examinations and establishment of local diagnostic reference levels. In *IFMBE Proceedings*. Springer Berlin Heidelberg, pp.860–863.
- Smith, L., Haque, M., Morales, J., Hill, R. and Smith, L. (2015). Radiation dose measurements of an on-board imager X-ray unit using optically-stimulated luminescence dosimeters. *Australasian Physical and Engineering Sciences in Medicine*. 38(4), 665–669.

- Suliman, I.I., Abbas, N. and Habbani, F.I. (2007). Entrance surface doses to patients undergoing selected diagnostic X-ray examinations in Sudan. *Radiation Protection Dosimetry*. 123(2), 209–214.
- Taha, M.T., Al-Ghorabie, F.H., Kutbi, R.A. and Saib, W.K. (2015). Assessment of entrance skin doses for patients undergoing diagnostic X-ray examinations in King Abdullah Medical City, Makkah, KSA. *Journal of Radiation Research and Applied Sciences*. 8(1), 100–103.
- Takegami, K., Hayashi, H., Okino, H., Kimoto, N., Maehata, I., Kanazawa, Y., Okazaki, T., Hashizume, T. and Kobayashi, I. (2016). Estimation of identification limit for a small-type OSL dosimeter on the medical images by measurement of X-ray spectra. *Radiological Physics and Technology*. 9(2), 286–292.
- Takegami, K., Hayashi, H., Okino, H., Kimoto, N., Maehata, I., Kanazawa, Y., Okazaki, T. and Kobayashi, I. (2015). Practical calibration curve of small-type optically stimulated luminescence (OSL) dosimeter for evaluation of entrance skin dose in the diagnostic X-ray region. *Radiological Physics and Technology*. 8(2), 286–94.
- Takegami, K., Hayashi, H., Yamada, K., Mihara, Y., Kimoto, N., Kanazawa, Y., Higashino, K., Yamashita, K., Hayashi, F., Okazaki, T., Hashizume, T. and Kobayashi, I. (2017). Entrance surface dose measurements using a small OSL dosimeter with a computed tomography scanner having 320 rows of detectors. *Radiological Physics and Technology*. 10(1), 49–59.
- Tamboul, J.Y., Yousef, M., Mokhtar, K., Alfaki, A. and Sulieman, A. (2014). Assessment of entrance surface dose for the patients from common radiology examinations in Sudan. *Life Science Journal*. 11(2), 164–168.
- Tawfik, G., Yunfeng, C., James, G., Yan, Y. and Ying, X. (2013). Surface dose measurements of kV XVI cone-beam CT system using nanoDot optically stimulated luminescence dosimeters. In M. Long, ed. *World Congress on Medical Physics and Biomedical Engineering May 26-31, 2012, Beijing, China*. IFMBE Proceedings. Springer Berlin Heidelberg, pp.1195–1198.
- Tsoufanadis, N. and Landsberger, S. (2011). *Measurement and detection of radiation* 3rd ed., London: CRC Press: Taylor & Francis Group.
- Twardak, A., Bilski, P., Marczevska, B. and Gieszczyk, W. (2014). Analysis of TL and OSL kinetics of lithium aluminate. In *Radiation Measurements*. pp.143–147.
- UNSCEAR (2011). Sources and effects of ionizing radiation. *UNSCEAR 2008 Report*



- to the General Assembly with Scientific Annexes C, D and E. Vol 2.*
- UNSCEAR (2010). Sources and effects of ionizing radiation. *UNSCEAR 2008 Report to the General Assembly with Scientific Annexes. Vol 1.*
- Viamonte, A., da Rosa, L.A.R., Buckley, L.A., Cherpak, A. and Cygler, J.E. (2008). Radiotherapy dosimetry using a commercial OSL system. *Medical Physics.* 35(4), 1261–1266.
- Vock, P. and Szucs-farkas, Z. (2009). Dual energy subtraction : Principles and clinical applications. *European Journal of Physics.* 72, 231–237.
- Wen, N., Guan, H., Hammoud, R., Pradhan, D., Nurushev, T., Li, S. and Movsas, B. (2007). Dose delivered from Varian’s CBCT to patients receiving IMRT for prostate cancer. *Physics in Medicine and Biology.* 52(8), 2267–76.
- Yahnke, C.J. (2009). MicroStar calibration and usage instruction. *Landauer inLight Systems.* Available at:  
[http://www.landauer.com/uploadedFiles/Resource\\_Center/microStar Calibration and Usage Instructions 10-Jun-09.pdf](http://www.landauer.com/uploadedFiles/Resource_Center/microStar%20Calibration%20and%20Usage%20Instructions%2010-Jun-09.pdf) [Accessed April 16, 2016].
- Yoo, W.J., Seo, J.K., Shin, S.H., Han, K.-T., Jeon, D., Jang, K.W., Sim, H.I., Lee, B. and Park, J.-Y. (2013). Measurements of entrance surface dose using a fiber-optic dosimeter in diagnostic radiology. *Optical Review.* 20(2), 173–177.
- Yoshimura, E.M. and Yukihiro, E.G. (2006). Optically stimulated luminescence: Searching for new dosimetric materials. *Nuclear Instruments and Methods in Physics Research, Section B: Beam Interactions with Materials and Atoms.* 250(1–2 SPEC. ISS.), 337–341.
- Yukihiro, E.G. and McKeever, S.W.S. (2011). *Optically stimulated luminescence: Fundamentals and Applications*, Oklahoma, USA: John Wiley & Sons.
- Yukihiro, E.G. and McKeever, S.W.S. (2008). Optically stimulated luminescence (OSL) dosimetry in medicine. *Physics in Medicine and Biology.* 53, R351–R379.
- Yukihiro, E.G., Ruan, C., Gasparian, P.B.R., Clouse, W.J., Kalavagunta, C. and Ahmad, S. (2009). An optically stimulated luminescence system to measure dose profiles in x-ray computed tomography. *Physics in Medicine and Biology.* 54(20), 6337–52.
- Yusuf, M., Saoudi, A., Alothmany, N., Alothmany, D., Natto, S., Natto, H., Molla, N.I., Mail, N., Hussain, A. and Kinsara, A.A. (2014). Characterization of the optically stimulated luminescence nanodot for CT dosimetry. *Life Science Journal.* 11(2), 445–450.